Roh, K.-M., Lühr, H., Rothacher, M., Park, S.-Y. (2009): Investigating suitable orbits for the Swarm constellation mission - The frozen orbit. - Aerospace Science and Technology, 13, 1, 49-58

DOI: 10.1016/j.ast.2008.03.001

Investigating suitable orbits for the Swarm constellation mission – The frozen orbit

Kyoung-Min Roh*, Hermann Luehr*, Markus Rothacher*, Sang-Young Park**

*GeoForschungsZentrum (GFZ) Potsdam, Telegrafenberg, D-14473 Potsdam, Germany

**Astrodynamics and Control Lab., Dept. Astronomy, Yonsei University, Seoul, 120-749, Republic of Korea

Abstract— This paper proposes a suitable orbit design for the lower pair of ESA's Swarm constellation mission, flying side-by-side in near-polar and circular orbits with a separation of only 1.4° at ascending node. Both orbits are suggested to be frozen orbits to minimize the evolution, and an along-track separation strategy is applied to avoid collision risk. The characteristics of the proposed orbit type are examined through numerical techniques including high-fidelity perturbation models. The prime change from the initial configuration is an along-track separation. The perturbations causing the along-track drift are analyzed by switching on/off certain perturbations. The results indicate that the tesseral harmonics and the atmospheric drag yield dominant effects. The atmospheric drag effect shows a dependence on the local time of the ascending node. From two months of orbit propagation for the altitude 300 km the maximum along-track drift we obtain is about 80 km, which is still within the measurement requirement range. Several maneuver strategies for maintaining the proposed orbit design are suggested. The results analyzed for the proposed orbit design show that collision risk can be avoided by along-track separation within the frozen orbit design. Consequently, this combination is considered as a suitable approach for Swarm's lower pair.

Keyword —constellation design, orbit maintenance strategy, frozen orbit

I. Introduction

Constellation missions are playing, nowadays, an increasing role for observations on global scales providing high spatial and temporal resolution at the same time. The term constellation referred to here means a group of satellites with a dedicated distribution in space, tailored to support the mission goals. Formation flight also requires a group of satellites, but it places more stringent requirements on the constellation. Satellites flying in a formation are kept at relative positions, maintaining a certain shape, e.g., a circle or line by moving on

neighboring orbits and by controlling the orbits tightly in order to keep the desired formation [1]. As an example, ESA's Earth Observation Mission Swarm can be considered as a constellation mission, it is investigated in detail in the present paper. The object of the Swarm mission is to provide a high-precision survey of the geomagnetic field and its temporal evolution. For achieving that the Swarm concept consists of a constellation of three satellites in three different near-polar orbits. One satellite will be operated at an initial altitude of 530 km and two satellites will start at a lower orbit height of about 450 km [2]. In order to achieve a high spatial resolution the lower pair will fly side-by-side at an inclination of 87.4° and with a difference in ascending node of only 1.4°. Ideally the two spacecrafts should cross a given latitude at the same time. This allows to obtain the east/west gradient of the magnetic field, not biased by temporal changes. Therefore, the lower set can be regarded as a formation flying. For practical reasons, a certain difference in latitude crossing time has to be maintained in order to avoid the risk of collision. From assessment of the variability of the geomagnetic field it was concluded that time difference up to 10 seconds can be tolerated for driving stable spatial gradients. For the higher satellite also a circular orbit is foreseen but with a somewhat larger inclination (88°). This inclination of the higher satellite is proposed to give a slightly slower drifting of the right ascension of the ascending node than the lower one. Over the 4 years of the mission life time the orbital planes will separate by 120°, providing the opportunity of sampling the geomagnetic field simultaneously at varying local time differences. Further details of the upcoming Swarm mission can be found at [2] and/or web site (http://www.esa.int/esaLP/LPswarm.html).

The orbits of the two lower satellites cross over near the poles, which may lead to a collision at these points. It is therefore necessary to implement a collision-avoidance strategy without violating the measurement requirements – same inclination, ascending node difference (1.4°), same semi-major axis, and small difference in the equator crossing time (<10sec) [2]. There are two possible approaches for avoiding collisions. The first method makes use of altitude differences at the poles by designing both orbits slightly elliptical and locating their perigees at the South and North Pole, respectively. The apparent disadvantage of this method is the rotation of the argument of perigee. After a few months the required altitude difference at the poles cannot be guaranteed anymore. A frozen orbit could be the solution since it prevents the argument of perigee from rotating. There exists, however, only one solution of a frozen orbit for Swarm's altitude and inclination. A simple combination of a frozen orbit with a circular orbit is also not a vital solution because, in practice, the circular orbit cannot maintain its eccentricity lower than the frozen eccentricity due to the perturbation caused by the zonal harmonics [3]. Resultantly, the hazard of collision is not eliminated by this altitude differencing

method. The other method and probably the more reliable strategy for avoiding a collision, is to maintain a separation between the spacecraft in along-track direction. When both orbits are designed as frozen orbits, the deformation of orbits can be minimized. The greatest advantages of frozen orbits are that the variations of their orbital parameters are minimized and the effort for orbit maintenance can be reduced [3-5]. Due to these advantages, many Earth observation missions like SEASAT-A, LANDSAT, GEOSAT, SPOT, ERS, Topex/Poseidon, were placed into a frozen orbit [4,5], and the orbit for a lunar mapping mission was designed in that way [6]. Here we assess the possibility of applying the frozen orbit concept also for the Swarm mission. The main goal of this study is to present a strategy for collision avoidance by allowing for some along-track separation and to examine the characteristics of the orbit evolution with respect to required maintenance.

The approach for collision-avoidance of Swarm's lower pair is based on the maintenance of an along-track separation. If the separation is too large (>100 km), it reduces the scientific value of the constellation measurements. Therefore, the purpose of this study is to present an orbit design that allows minimizing the along-track distance without risking a collision. The satellites in the lower constellation will experience different perturbations, especially due to the tesseral harmonics and due to differences in atmospheric drag, even though the two spacecrafts are flying closely together. Thus the evolution of the initial configuration has to be examined. For this task we use a high-precision orbit propagation software for numerically analyzing the evolutions of the orbital elements and the relative separation of the two satellites.

In section 2 we first introduce the mathematical frame work for designing a frozen orbit. In section 3 we present the characteristics of a frozen orbit for Swarm's lower pair. Section 4 focuses on the evolution of the Swarm frozen orbits under realistic orbital conditions. An idea on the correction maneuvers for maintaining a frozen orbit over long times is given in Section 5. Finally, the results are summarized in the Conclusion section.

II. Frozen orbit concept

The term frozen orbit stands for an orbit type where the mean argument of perigee, the eccentricity, and the inclination are kept constant. Generally, the changes in eccentricity and argument of perigee are caused mainly by zonal harmonics of the Earth's gravity field [3]. Specifically, even zonal harmonics cause secular variations, and odd zonal harmonics cause long-term variations. However, under special conditions the secular variations due to the J2 term can be nullified by the odd zonal harmonics of the Earth's gravity field. The term 'frozen orbit' was introduced by Cutting et al. in 1978 in their work on the analysis of the SEASAT-A orbits [7]. The frozen condition can be achieved by setting the secular variation of eccentricity and argument of perigee to

zero, and it has originally been analyzed by Cook in 1966 [8].

Before introducing Cook's analysis, which is used in this study for finding the frozen conditions, we will briefly review the simple frozen conditions. These are helpful for understanding the principles of frozen conditions which are based on the time derivatives of the argument of perigee, inclination and of the eccentricity. Considering only J_2 and J_3 perturbation terms we obtain [5,6]

$$\frac{de}{dt} = \frac{-3J_3 n}{2(1-e^2)^2}\left(\frac{R_e}{a}\right)^3 \sin I_0 \left(1-\frac{5}{4}\sin^2 I_0\right)\cos\omega \tag{1}$$

$$\frac{di}{dt} = \frac{-3J_3 n}{2(1-e^2)^3}\left(\frac{R_e}{a}\right)^3 e\cos I_0 \left(1-\frac{5}{4}\sin^2 I_0\right)\cos\omega \tag{2}$$

$$\frac{d\omega}{dt} = \frac{3J_2 n}{(1-e^2)^2}\left(\frac{R_e}{a}\right)^2 \left(1-\frac{5}{4}\sin^2 I_0\right)F \tag{3}$$

where, a, e, I_0, and ω are orbital elements referring to semi-major axis, eccentricity, inclination, and argument of perigee, respectively, n is the mean motion, and R_e is the mean equatorial Earth radius. F is given by

$$F = 1+\frac{J_3}{2J_2(1-e^2)}\left(\frac{R}{a}\right)\left(\frac{\sin^2 I_0 - e^2\cos^2 I_0}{\sin I_0}\right)\frac{\sin\omega}{e} \tag{4}$$

Two frozen conditions can be derived from the above equations. The first explicit frozen condition is achieved when the factor $\{1-(5/4)\sin^2 I_0\}$ is zero. Namely, at an inclination of 63.4° or 116.6°, the so called 'critical inclination', an orbit becomes frozen. Another frozen condition can be derived at ω = 90° or 270°. Namely, the variation of the mean eccentricity and inclination (cf. Eq. (1) and (2)) becomes zero, and an eccentricity, the so called 'frozen eccentricity' that nullifies the long-term variation of the argument of perigee, can be achieved by setting F to zero. Therefore, there are two types of frozen orbits. The former is an orbit at the critical inclination, and the latter is an orbit whose argument of perigee points either to the South or to the North Pole with the frozen eccentricity. The location of the perigee depends on the signs of J_2 and J_3, i.e., if both have the same sign ω = 270°, and if different, ω = 90° [4].

Design of a frozen orbit

For a mission with dedicated inclination, like Swarm, only the latter approach of a frozen orbit can be applied. In this study the analytical frozen eccentricity solution developed by Cook is used because this solution is expressed by using transformed variables instead of classical elements, in order to prevent singularities, and it takes into account the high odd zonal harmonic terms [8]. It also helps to better understand the evolution of an orbit at near-frozen condition. Here, we only repeat the relevant formulae for a frozen eccentricity. The detailed derivation can be found in [8]. The Cook's method starts from the fact that the rate of change of e and ω due to disturbing forces can be described by Lagrange's equation. Only the Earth's gravitational potential expressed in terms of spherical harmonics is considered here as the disturbing function [8]. The time derivatives of e and ω are the transformed time derivatives of new variables ξ (= $e\cos\omega$) and η (= $e\sin\omega$). Therefore, the derivative equations of ξ and η, considering the gravitational harmonics, can be expressed as

$$\begin{aligned} \dot{\xi} &= -k\eta + C \\ \dot{\eta} &= k\xi \end{aligned} \tag{5}$$

and the solutions of ξ and η have the following form

$$\begin{aligned} \xi &= e_0 \cos(kt + \omega_0) \\ \eta &= e_0 \sin(kt + \omega_0) + C/k \end{aligned} \tag{6}$$

where, e_0 and ω_0 are the initial eccentricity and argument of perigee. The variable *k* and the explicit form of *C* considering odd harmonic terms up to J_9 are given by [8]

$$k = 3nJ_2\left(\frac{R_e}{a}\right)^2\left(1-\frac{5}{4}f\right) \tag{7}$$

$$\begin{aligned} C = -\frac{3}{2}n\left(\frac{R_e}{a}\right)^3 \sin I_0 \Bigg\{ & J_3\left(1-\frac{5}{4}f\right) - \frac{5}{2}J_5\left(\frac{R_e}{a}\right)^2\left(1-\frac{7}{2}f+\frac{21}{8}f^2\right) \\ & + \frac{35}{8}J_7\left(\frac{R_e}{a}\right)^4\left(1-\frac{27}{4}f+\frac{99}{8}f^2-\frac{429}{64}f^3\right) \\ & - \frac{105}{16}J_9\left(\frac{R_e}{a}\right)^6\left(1-11f+\frac{143}{4}f^2-\frac{715}{16}f^3+\frac{2431}{128}f^4\right)\Bigg\} \end{aligned} \tag{8}$$

where, $f = \sin^2 I_0$. For this initial mission design purpose, it is enough to include odd harmonics up to J_9. According to Fig. 1 in Cook's literature [8], Eq. (6) indicates that the ξ and η perform a circular motion with radius e_0 about the center $(0, C/k)$ in the (ξ, η) plane with a period of $2\pi / k$. This circular motion means that a mean eccentricity oscillate with an amplitude of $|e_0 - C/k|$. An evolution of the argument of perigee is depends on the initial eccentricity whether it is bigger than the frozen value or not. The detailed motion can be referred in Ref. [5] and Ref. [8]. By the way, if the eccentricity (e_0) has the value of C/k, then neither the eccentricity nor the argument of perigee oscillate. Therefore the value C/k is called the frozen eccentricity. The mean eccentricity cannot be lower than the frozen value because it circulates around the frozen eccentricity. Figure 1 shows the frozen eccentricity as a function of orbital inclination from 0° to 90° for an altitude of 450 km which is valid for Swarm's lower pair. The zonal harmonic terms given in the legend represents the upper limit of terms taking into account for calculating the frozen eccentricity. It can be seen that the frozen eccentricity varies rapidly near the critical inclination, 63.4°, from lower to higher inclinations.

III. A Case Study: the Swarm lower pair

Design of a frozen orbit for Swarm

The Swarm mission is composing of three satellites, one at higher initial altitude of 530 km and two at lower altitude of 450 km. The lower set has an inclination of 87.4° with a 1.4° separation of the ascending nodes. The frozen eccentricity for the orbits of the lower pair has been calculated using Eq. (7) and Eq. (8), and the dependencies of the frozen eccentricity on zonal-terms, inclination, and altitude have been investigated. Note that the altitude dependence has been examined for a range from 450 km to 300 km because the altitude of the lower constellation decays from 450 km in the initial phase to 300 km at the end of mission.

First, the frozen eccentricities are calculated for an inclination of 87.4° and a 450 km altitude, taking into account different degrees of zonal harmonics. The results are listed in Table 1. The frozen eccentricity becomes larger when the considered harmonic degrees are increased. This property can also be seen in Figure 1 and the dependence on zonal terms is higher for near-polar orbits than for lower inclination orbits. The effects of different levels of frozen eccentricity are verified in the next section through numerical orbit propagation. The dependencies on inclination and altitude are also plotted in Figure 2 and Figure 3, respectively, and it is shown that only small changes in eccentricity are required within the altitude range of 450 km to 300 km.

Verification of frozen eccentricity

The frozen properties, i.e., constant mean eccentricity, inclination, and argument of perigee, can be violated because there are lots of perturbations affecting orbital elements besides the non-symmetric Earth gravity terms. So the analytically calculated frozen eccentricities for the Swarm mission are verified here through a high-precision orbit propagator. To perform numerical verification we use the Adams-Cowell predictor/corrector of 11th order for the numerical integration, the EGM 96 model (up to a degree and order 70×70) for perturbations due to the non-symmetrical Earth gravity field, the NRLMSIS-00 model for the atmospheric density [9], the HWM93 model for high altitude wind velocity [10], and the DE405 JPL coefficient for the lunar/solar ephemeris **[**11**]**. Perturbations due to atmospheric drag, lunar/solar gravitational attraction, solid Earth and ocean tides [12], and solar radiation pressure are also included. When atmospheric drag and solar radiation pressure perturbations are calculated, a triangular prism-type of macro model is employed for the spacecraft of the Swarm mission and a three-axis stabilized nadir pointing attitude is assumed [13]. Finally, the achieved frozen values are the mean orbital elements, so the initial osculating orbital elements for the numerical integration are calculated using Kozai's orbit theory [14]

Numerical orbit propagations have been conducted with various levels of perturbations and frozen eccentricities. The secular variation of orbital elements has been calculated using orbit runs over 60 days from 1 January 1999, 12h onward. The epoch is chosen for matching the solar cycle phase of the Swarm mission's expected period. The initial mean orbital elements are set at 450 km altitude, 87.4° inclination, and 0° right ascension of ascending node. The results are summarized in Table 2. It can be seen that the variation of eccentricity and argument of perigee are affected by different degrees of perturbation terms, and their frozen properties are more distinct when the higher zonal terms are taken into account. By the way, when all considered perturbations are included, the variation of the inclination is 10 times higher than in the case where only the gravity model is included. The reason of this increase is that the sun-moon attraction causes a long-term variation in inclination [3]. The frozen properties can be seen more explicitly in Figure 4 which shows the osculating elements e and ω over four weeks. In Figure 4 the osculating elements move around the mean point with two circular loops and wings [15]. However, when different levels of perturbations are considered, the width of the osculating elements' variation is getting larger for the low zonal terms. This width means the amplitude of the mean eccentricity's variation. Namely, if an initial eccentricity is near the frozen value, the mean eccentricity will oscillate about the frozen value with about a period of about $360 \text{ deg}/\dot{\omega}$ as

shown in Eq. (6), where $\dot{\omega}$ is the secular rate due to J_2. The time during which the eccentricity is larger than the frozen value is longer than when it is smaller than the frozen value. This means that the average eccentricity is always higher than the frozen value [3]. Thus, it can be concluded that a frozen eccentricity is the lowest mean eccentricity that can be maintained in an actual mission operation. These results also demonstrate that the collision avoidance approach by maintaining altitude differences at the poles (i.e., using two elliptical orbits or the combination of a frozen and a circular orbit) is not a practical solution.

In summary, the frozen orbit for the lower pair of the Swarm spacecraft is outlined by analytical methods and its dependencies on zonal terms, inclination, and altitude are examined by numerical simulations. In the case of the Swarm mission, the frozen orbit is only applicable for ω =90°, and its eccentricity does not vary significantly within the altitude range of 300 km to 450 km. The results from the high-precision numerical analysis show that the rate of change of ω is 0.025°/day which is about 1 % of the typical change in argument of perigee for a circular orbit at Swarm's altitude and inclination.

IV. Relative separations of the lower Swarm satellites

To examine the proposed collision avoidance approach, i.e., an along-track separation strategy, the relative separation of the two lower satellites and its evolution are examined by numerical simulation. The same orbit propagator as in the previous section is used for this task. Both lower orbits are designed as frozen with the same altitude and inclination. By positioning the two satellites simultaneously at the equator the angular separation between the two satellites becomes 0.00635°, as shown in Figure 5, and this angular separation corresponds to about 7.5 km of along-track separation at the cross-over point..

Evolution of the relative separation

The orbit of the lower pair will decay from 450 km altitude to 300 km at the end of the mission. So, to cover the whole Swarm mission period, simulations are conducted for three phases at different altitude and epochs, 450 km, 375 km, and 300 km at the beginning of 2000, 2002, and 2004, respectively. The local time of the ascending node (LTAN) is set to 12h. The effect of the LTAN will be analyzed later. Since Swarm is scheduled to be launched end of 2010, our initial epoch is set to 1 January 2000 (i.e., one solar cycle earlier) in order to have similar orbital environment conditions for the simulation. The initial epoch and mean orbital elements for each simulation and the resulting rates of secular variation of the orbital elements are summarized in Table 3 and Table 4, respectively.

For Phase-1 the distances between the two satellites along the three principal directions is shown in Figure 6 for five orbits starting at the North Pole. As seen in Figure 6, the values of the radial and along-track separations are almost constant with small fluctuations. Because the collision risk occurs only at the poles, the position difference at the poles is of concern here. Thus the y-axis of Figure 6 is limited to ±50 km intentionally because the maximum cross-track separation occurs only at the equators. The maximum separations are about 2 km in radial direction, 7.5 km for the along-track, and 170 km for the cross-track component. The decomposed separations for Phase-2 and Phase-3 are similar in shape to those of Phase-1. The secular variations of the two frozen orbits are slightly different except for the change of the ascending node, as shown in Table 4. There are a lot of factors that make the two satellites experience different perturbations like atmospheric drag and tesseral harmonics. In reality, there are more factors expected which cause deviations from our orbit design, like different ballistic coefficient between spacecrafts and individual spacecraft attitudes. As seen in Figure 7, the along-track drift has to be considered as a representative deviation from the initial design. While the along-track drift during 60 days in Phase-1 is about 20 km, the radial drift is just about 60 m. The radial and along-track drift is getting larger up to 600 m and 80 km, respectively, as the altitude becomes lower to 300 km. The maximum differential delay in equator crossing is specified to be less than 10 seconds, which corresponds to about 75 km for the altitude of the lower pair. The along-track separation of Phase-3 in 60 days exceeds the measurement requirement by about 5 km.

Along-track drift

The results of the previous section indicate that the along-track drift is the dominant change deforming the proposed constellation design. The factors that cause the along-track drift are mainly atmospheric drag and tesseral harmonics [16]. The along-track drift is a very critical problem for formation flying missions, especially when along-track separation requirements are tight like for synthetic aperture radar missions [17]. Numerical simulations taking into account different degrees of perturbations are conducted to provide physical insight into the changes of the proposed orbit design.

First, the along-track drift calculated in the previous section is compared with the results achieved for the cases when all perturbations are turned off except the perturbations due to the non-symmetrical geopotential and the atmospheric drag. We have investigated three cases (1) using for the geopotential only 20 degrees of the zonal harmonics, (2) considering a 20×20 geopotential, and (3) adding atmospheric drag to the 20×20 geopotential. The along-track drift calculated from different degrees of perturbation models are compared in

Figure 8 for the three mission phases. The integration period is reduced to 30 days in this subsection, because there are lots of unexpected factors in reality, influencing in particular the along-track orbit. As seen in Figure 8, the dominant perturbations inducing an along-track drift are the high order tesseral harmonics and atmospheric drag. While the along-track drift due to tesseral harmonics (up to order 20) is in the range of 12 to 16 km over 30 days for all three phases (dashed line), the effect of atmospheric drag is getting stronger as the altitude becomes lower (dashed-dotted line). While the along-track drift during Phase-1 increases by only about 5 km in one month when adding the atmospheric drag to the gravity perturbation, the along-track drift during Phase-3 increases by about 20 km over the same period. In reality, the effect of atmospheric drag is much more uncertain than suggested by our numerical test because many factors like spacecraft attitude, cross-section, and mass will influence the atmospheric drag effect.

The dependence of the along-track drift on the local time of the ascending node (LTAN) is also examined for the three different phases of the previous section. The same orbital elements as in Table 3, except for the ascending node, are used. The changes in along-track separation after an orbit propagation of 30 days are plotted versus LTAN in Figure 9. A distinct property emerging from Figure 9 is that the direction and the amplitude of the along-track drift have a symmetrical form with respect to the LTAN except for Phase-1. This implies that atmospheric drag causes the symmetry because of its' high dependency on the LTAN [18]. Though the sun-moon attraction and the solar radiation pressure are also effected by LTAN, but their effects are revealed as ignorable in this case, as seen in Figure 8. So it may be concluded that the dependence of the along-track drift on LTAN comes primarily through atmospheric drag. For that reason Phase-1 shows a less symmetric pattern because of the dominance of tesseral harmonics over atmospheric drag. The maximum along-track drifts occur at 0 hour, and at 12 hour LTAN with positive direction, i.e., S/C–A is ahead of S/C–B. At 6 hour, and at 18 hour LTAN we find maximum along-track drifts with negative direction. In all the tests, no case was found which violates the separation requirement of the Swarm lower pair within one month. In case of negative along-track drift, the separation approaches zero. However, collision can be prevented by setting S/C-A behind S/C-B.

In summary, the lower pair of Swarm spacecraft is required to maintain the equator crossing time difference within 10 seconds, i.e., along-track distance < 75 km. All test cases show that this requirement can be maintained over 30 days. However, at low altitude, where Swarm will be operated near the end of the mission, the along-track separation increases up to 80 km after 60 days. The main factors causing the along-track drift of the Swarm lower pair are tesseral harmonics and atmospheric drag. In particular, the dependence on

atmospheric drag is related to LTAN, so the maximum along-track drifts occur around 0h and 12h in positive direction, and 6h and 18h in negative direction.

V. Strategy for correction maneuvers

The results of the previous chapters show that the proposed orbit design i.e., frozen orbit is very stable, so the evolution of the orbit is more expectable than a non-frozen orbit. Collision avoidance strategy using along-track separation also shows that the measurement requirements of the Swarm lower pair are maintained for nearly 60 days even at 300 km, the lowest operational altitude of Swarm. This stability helps to extend the mission life time by reducing fuel usage for constellation maintenance. However, the along-track drift should be controlled carefully in order to maintain the measurement requirements of the Swarm lower pair. The along-track drift induced by the perturbations of tesseral harmonics and atmospheric drag can be controlled through corrections in the semi-major axis of the satellites. With the help of Gauss' variational equations of motion, the change of the semi-major axis (Δa) due to a small impulse in tangential direction (Δv_t) can be expressed by [19]

$$\Delta a = \frac{2a^2}{\mu}\Delta v_t \tag{9}$$

where μ stands for the gravitational constant times the mass of the Earth ($= GM$). Based on the above equation, the amount of velocity change, namely the fuel required to reduce the along-track drift, can be estimated. To change the semi-major axis during Phase-1 by 1 m, the required velocity increase is about 0.56 mm/sec. This impulse results in a change of the along-track separation by about 3.14 m per revolution.

Maneuvers to maintain the frozen orbit may also be required in spite of its stability over a long time, as seen in Section III, because the orbit may experience other perturbations in addition to those from zonal harmonics. The maneuver into a frozen orbit is usually understood as changing the eccentricity vector defined by the variables (ξ, η) of Eq. (5), i.e., the maneuver from an arbitrary eccentricity vector to the frozen one (0,*C*/*k*). Generally, a two-impulse maneuver is employed to change the eccentricity vector without changing the semi-major axis and inclination [20]. However, if a maneuver is required only for an argument of perigee change, single- and double-impulse transfers can be employed. When the rotation of the argument of perigee is $\Delta\omega$, then the sum of the two impulses is given by [3]

$$\Delta v_{\min} = e \cdot v_{r=p} \cdot \sin \frac{\Delta\omega}{2} \tag{10}$$

where $v_{r=p}$ is the velocity of a spacecraft at a true anomaly of 90°. This two-impulse value is half the velocity change of the single impulse maneuver. If $\Delta\omega$=30°, the required impulse is about 2.78 meter/sec. Note that the optimal point for the first impulse is at $\omega = 90° + \Delta\omega/2$ and the second impulse point is 180° away. A single-impulse strategy is also possible if the deviation from the frozen condition is not too large and if the change of semi-major axis due to the impulse is negligible [5]. The minimum impulse velocity ($\Delta v_{\min}$) can be expressed as a function of the initial and final frozen conditions [5],

$$\Delta v_{\min} = (v/2)\sqrt{e_i^2 + e_f^2 - 2e_i e_f \sin\omega_i} \tag{11}$$

where v is the along-track velocity, (e_i, ω_i) and $(e_f, \omega_f = 90°)$ are the initial and final eccentricities and arguments of perigee. For Phase-1, the minimum impulse velocity is calculated using Eq. (11) and plotted in Figure 10. Note that this single-impulse strategy can only be used if the maneuver is performed by both of the lower pair spacecraft at nearly the same time.

Maneuvers for maintaining the frozen conditions and controlling the along-track separation are introduced and some methods have been presented above. If the maneuver is performed during small deviations from the frozen condition, a suitable orbit maneuver can be performed with a single-impulse while generally two-impulse maneuvers are better. The along-track drift can be controlled by a small adjustment of the semi-major axis.

VI. Conclusion

A suitable orbit design for the lower satellite pair of the Swarm mission is presented in this paper. The along-track separation strategy is suggested for overcoming the collision hazard between two satellites flying side-by-side. The frozen orbit design is applied to both satellites of the lower pair to minimize the deformation of the initial orbit configuration. Frozen conditions are calculated using analytical formulae which take into account the zonal harmonics of the gravity field up to degree 9. The verification of the results through

high-fidelity orbit propagation software indicates that the secular variation of the eccentricity and the argument of perigee under the frozen condition are approximately of the order of 10^{-7}/day and 10^{-3}deg/day, respectively, which is about one-hundredth of the other elliptical orbits with the same semi-major axis. When phasing the two satellites in such a way that they cross the equator simultaneously, the initial along-track separation is about 7.5 km.

The proposed orbit design is tested for three different phases of the Swarm mission schedule, ranging from the initial altitude of 450 km at the epoch 2000 to the final 300 km altitude at the epoch 2004. The tested results show that the designed orbit approach can avoid the collision hazard, and the initial configuration is maintained for at least two months without violating the measurement requirements. After two month of orbital propagation the only major change is the along-track separation. The reasons of this separation are the tesseral harmonics and the atmospheric drag. The effect of the atmospheric drag is getting stronger as the altitude is getting lower, and at the same time it is depending on the local time of the ascending node. The maximum along-track drifts occur in noon-midnight and dawn-dusk orbits. It can be concluded that the orbit design proposed for the lower pair of Swarm satellites maintains its initial configuration for at least 2 months without any collision risk and without any need for maneuvers.

Finally, the required maneuver size to overcome the along-track separation is estimated by using Gauss' variational equations of motion. A one-metre change of the semi-major axis causes about 3 metres of along-track separation per revolution. A method to maintain the frozen condition is also presented, and the required velocity for a maneuver to reach a frozen orbit is about 3 meter/seconds if the deviation of the argument of perigee is about 30°.

Acknowledgement

Two of the authors (K-M. Roh and S-Y. Park) is supported by the Korea Science and Engineering Foundation (KOSEF) through the National Research Lab. Program funded by the Ministry of Science and Technology (No. M10600000282-06J0000-28210).

References

[1] A. C. Kelly, W. F. Case, Flying The Earth Observing Constellations, SpaceOps 2004, Eighth International Conference on space Operations, May 17 2004, Montreal, Canada, Paper No. 613-409.

[2] R. Haagmans, Swarm – The Earth's Magnetic Field and Environment Explorers, ESA Publications Division, ESA SP-1279, 2004.

[3] V. A. Chobotov, Orbital Mechanics, American Institute of Aeronautics and Astronautics, Inc., Washington, 1991, pp. 251-252, 291-296.

[4] B-S. Lee, J-S. Lee, Selection of Initial Frozen Orbit Eccentricity and Evolution of the Orbit Due to Perturbation, Journal of Korea Aeronautics and Space Sciences 25 (1) (1997) 126-132.

[5] M. Aorpimai, P. L. Palmer, Analysis of Frozen Conditions and Optimal Frozen Orbit Insertion, Journal of Guidance, Control, and Dynamics 26 (5) (2003) 786-793.

[6] S-Y. Park, J. L. Junkins, Orbital Mission Analysis for a Lunar Mapping Satellite, The Journal of the Astronautical Sciences 43 (2) (1995) 207-217.

[7] E. Cutting, G. H. Born, J. C. Frautnick, Orbit Analysis For SEASAT-A, Journal of the Astronautical Sciences 26 (4) (1978) 315-342.

[8] G. E. Cook, Perturbations of Near-Circular Orbits by the Earth's Gravitational Potential, Planet and Space Science 14 (1966) 433-444.

[9] J. M. Picone, A. E. Hedin, D. P. Drob, A. C. Aikin, NRLMSISE-00 empirical model of the atmosphere: Statistical comparisons and scientific issues, Journal of Geophysical Research (Space Physics), 107 (12) (2002) 1468-1484.

[10] A. E. Hedin, E. L. Fleming, A. H. Manson, F. J. Schmidlin, S. K. Avery, R. R. Clark, S. J. Franke, G. J. Fraser, T. Tsuda, F. Vial, R. A. Vincent, Empirical wind model for the upper, middle and lower atmosphere, Journal of Atmospheric and Terrestrial Physics 58 (1996) 1421-1447.

[11] E. M. Standish, JPL Planetary and Lunar Ephemerids, DE405/LE405, JPL IOM 312, 1998, F-98-048

[12] D. C. Christodoulidis, D. E. Smith, R. G. Williamson, S. M. Klosko, Observed Tidal Braking in the Earth/Moon/Sun System, Journal of Geophysical Research, 93 (B6) (1988) 6216-6236.

[13] J. A. Marshall, S. B. Luthcke, Modeling Radiation Forces Acting on Topex/Poseidon for Precision Orbit Determination, Journal of Spacecraft and Rocket 31 (1) (1994) 99-105.

[14] Y. Kozai, The motion of a close Earth satellite, The astronomical Journal, 64 (1959) 367-377.

[15] H. J. Rim, B. E. Schutz, C. E. Webb, P. Demarest, A. Herman, Repeat Orbit Characteristics and Maneuver Strategy for a Synthetic Aperture Radar Satellite, Journal of Spacecraft and Rockets, 37 (5) (2000) 638-644.

[16] C. Sabol, R. Burns, C. A. McLaughlin, Satellite Formation Flying Design and Evolution, Journal of Spacecraft and Rockets 38 (2) (2001) 270-278.

[17] S. D'Amico, O. Montenbruck, C. Arbinger, H. Fiedler, Formation Flying Concept for Close Remote Sensing Satellites, 15th AAS/AIAA Space Flight Mechanics Conference, Colorado, USA, Jan. 23-27, 2005, AAS 05-156.

[18] O. Montenbruck, E. Gill, Satellite Orbits, Models, Methods, and Application, Springer-Verlag, Berlin, 2000, pp. 87-88.

[19] R. H. Battin, An Introduction to the Mathematics and Methods of Astrodynamics, AIAA Education Series, AIAA, Washington, DC, 1987, pp. 484-490.

[20] B. Jones, Optimal Rendezvous in the Neighborhood of a Circular Orbit, Journal of Astronautical Sciences 41 (3) 55-90.

Table 1. Eccentricity of Swarm's lower pair orbits

Odd zonal Harmonics up to	Eccentricity
J_3	$e_{J3} = 0.00109125296$
J_5	$e_{J5} = 0.00120001617$
J_7	$e_{J7} = 0.00134235332$
J_9	$e_{J9} = 0.00140951039$

Table 2. Secular variation of the orbital elements when a frozen eccentricity is applied

	Δa (m/day)	Δe (/day)	Δi (°/day)	$\Delta\Omega$ (°/day)	$\Delta\omega$ (°/day)
Only Gravity 20×20(J_9)	0.0222	-0.293×10^{-6}	0.903×10^{-5}	-0.354	0.027
Only Gravity 70×70(J_9)	0.0232	-0.485×10^{-6}	0.896×10^{-5}	-0.355	0.035
All perturb. with e_{J3}	-15.85	8.850×10^{-6}	9.964×10^{-5}	-0.354	-0.405
All perturb. with e_{J5}	-15.87	5.746×10^{-6}	9.966×10^{-5}	-0.354	-0.251
All perturb. with e_{J7}	-15.90	1.653×10^{-6}	9.968×10^{-5}	-0.354	-0.063
All perturb. with e_{J9}	-15.92	-2.902×10^{-6}	9.968×10^{-5}	-0.354	0.025
All perturb. with e=0.	-15.71	3.627×10^{-5}	9.948×10^{-5}	-0.354	-2.023

Table 3. Initial orbital elements of Swarm's lower pair for the three considered phases

	Phase-1		Phase-2		Phase-3	
	Jan. 1. 2000, 12h		Jan. 1. 2002, 12h		Jan. 1. 2004, 12h	
	S/C A	S/C B	S/C A	S/C B	S/C A	S/C B
Altitude.	450 km		375 km		300 km	
e	0.0014095104		0.0014387735		0.0014695338	
Ω	280.461°	281.861°	280.969°	282.369°	280.491°	281.891°
i =87.4° , ω =90.0°, and Mean Anomaly=0.0°						

Table 4. Variation of orbital elements of Swarm's lower pair for the three phases

	Phase-1 Jan. 1. 2000, 12h		Phase-2 Jan. 1. 2002, 12h		Phase-3 Jan. 1. 2004, 12h	
	S/C A	S/C B	S/C A	S/C B	S/C A	S/C B
Δa (m/day)	-22.6	-22.6	-130.4	-130.6	-203.0	-203.2
Δe	-4.97×10^{-7}	-5.21×10^{-7}	-4.57×10^{-7}	-4.63×10^{-7}	-1.13×10^{-7}	-1.37×10^{-7}
Δi (deg/day)	-1.01×10^{-4}	-1.02×10^{-4}	-1.14×10^{-4}	-1.15×10^{-4}	-1.23×10^{-4}	-1.24×10^{-4}
$\Delta\Omega$ (deg/day)	-0.355	-0.355	-0.370	-0.370	-0.385	-0.385
$\Delta\omega$ (deg/day)	-3.62×10^{-2}	-1.45×10^{-3}	-3.08×10^{-2}	-3.04×10^{-2}	-3.42×10^{-2}	-3.12×10^{-2}

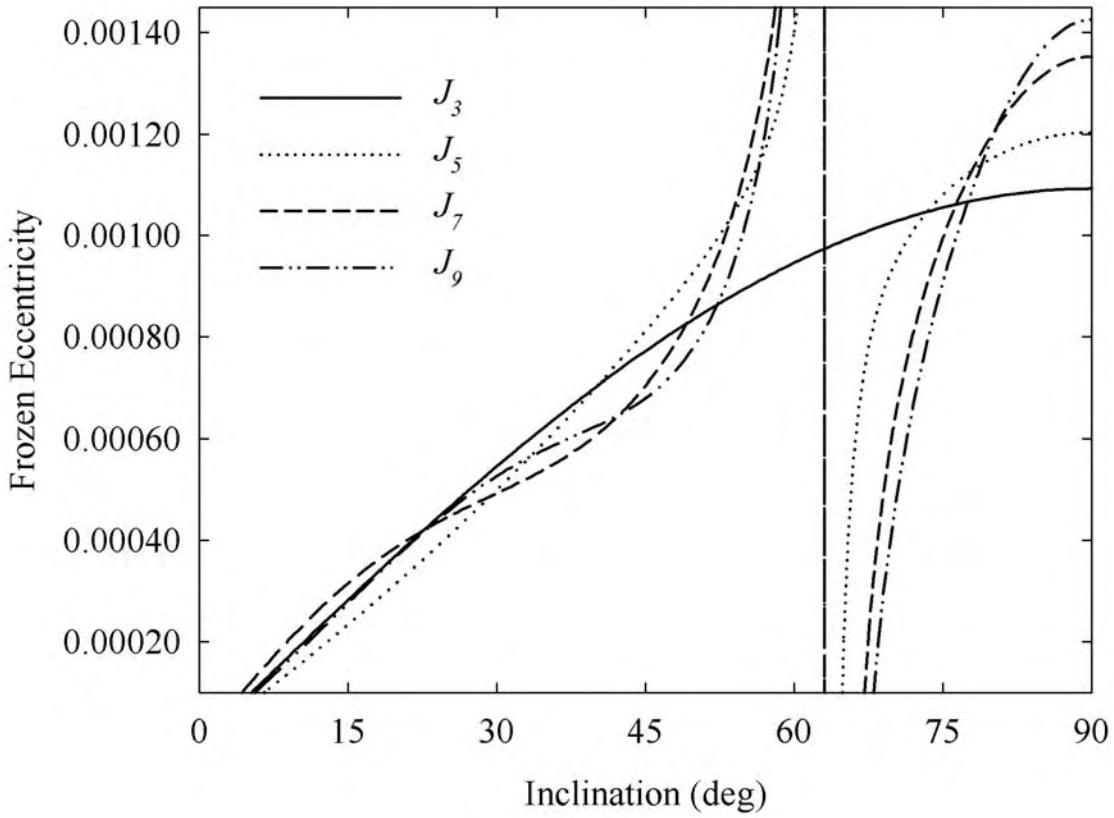

Figure 1. Eccentricity as a function of inclination for an altitude of 450 km. Zonal harmonics up to the indicated degree are considered.

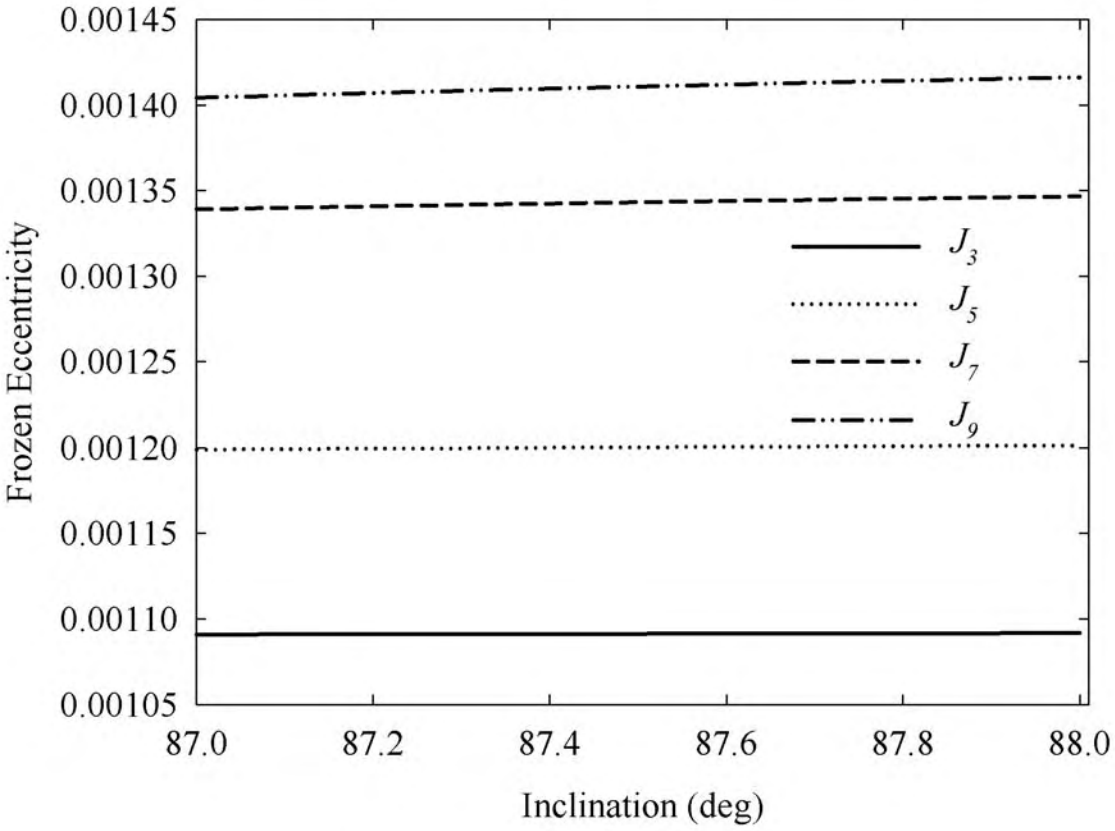

Figure. 2 The same of Figure 1, but for various inclinations near 87.4° and an altitude of 450 km.

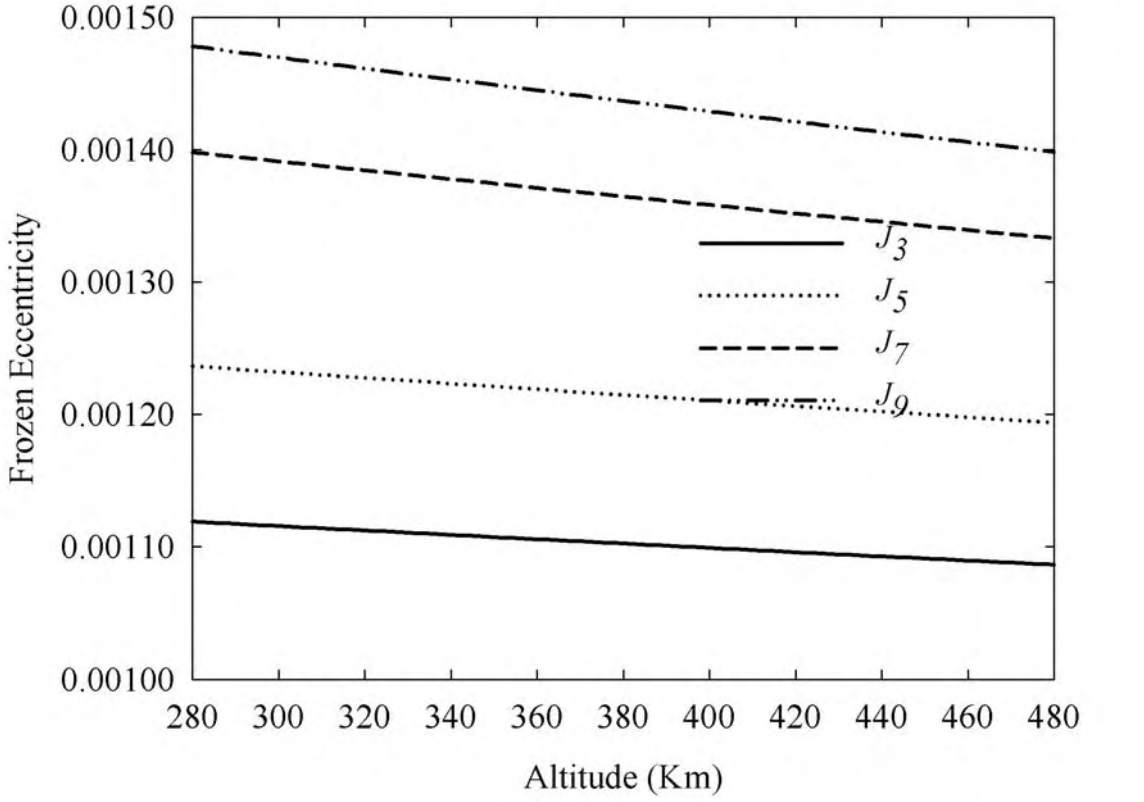

Figure 3. The same as Figure 1, but for an altitude range from 300 km to 450 km and an inclination of 87.4°.

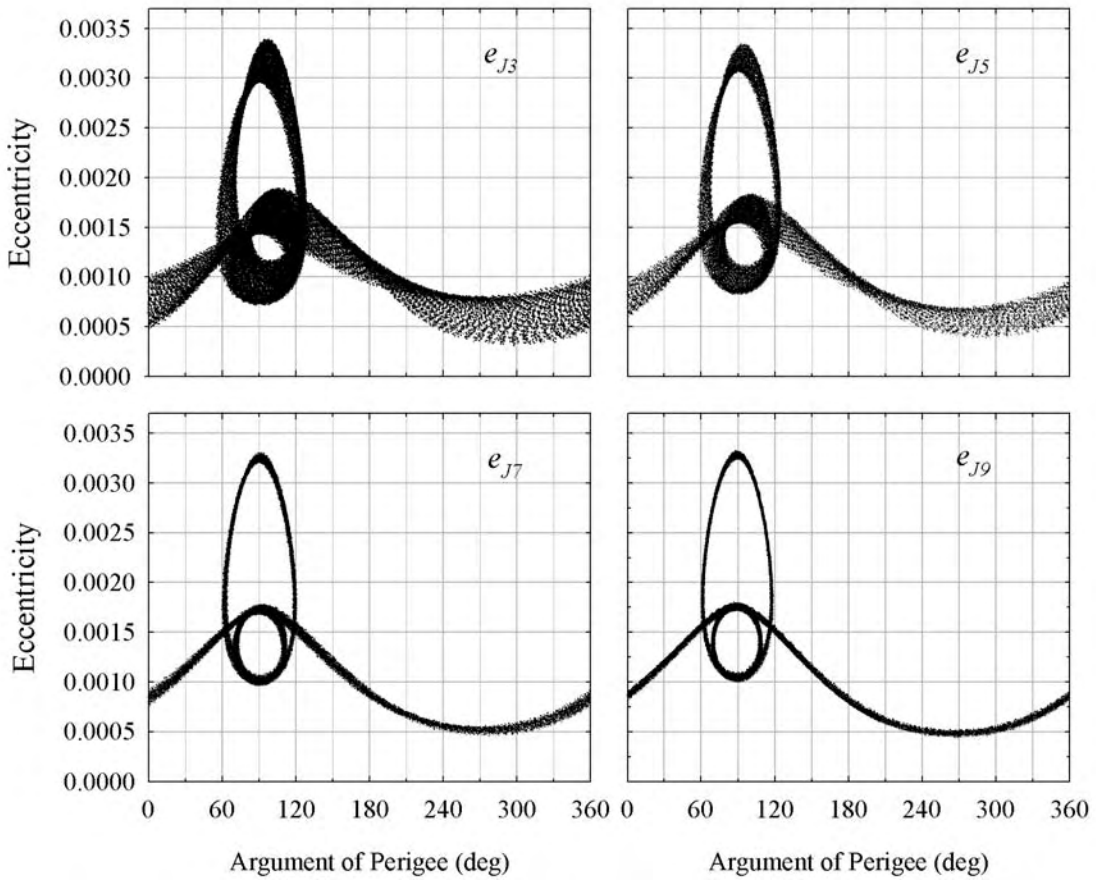

Figure 4. Motion of the osculating eccentricity and argument of perigee over 4 weeks. Zonal harmonics up to the indicated degree are considered.

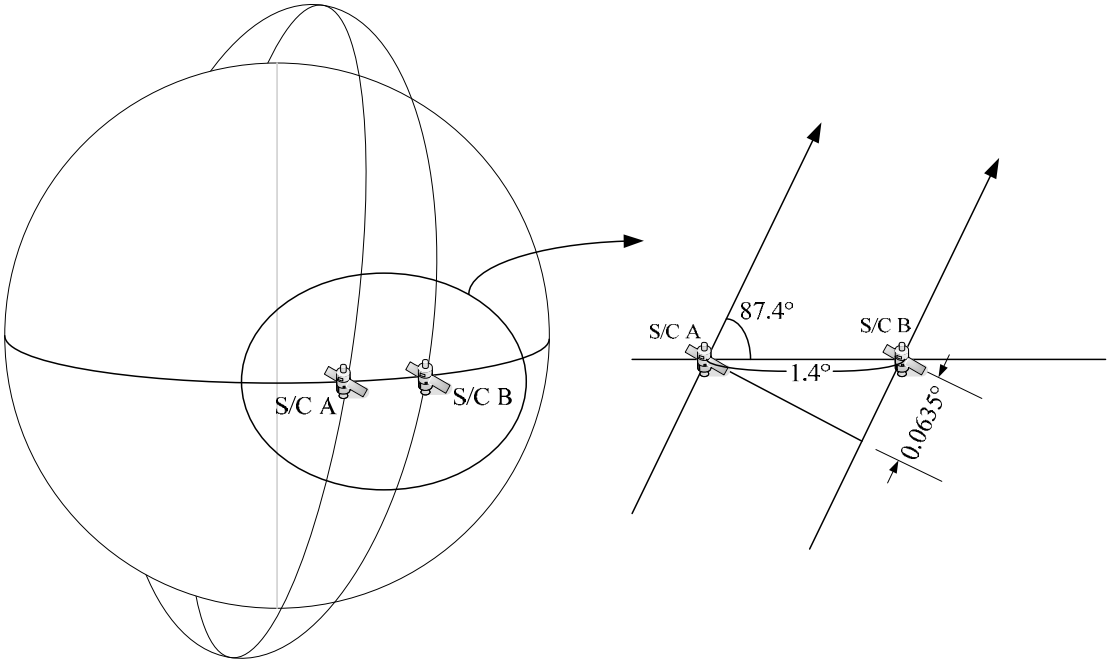

Figure 5. Along-track phasing of Swarm's lower pair satellites.

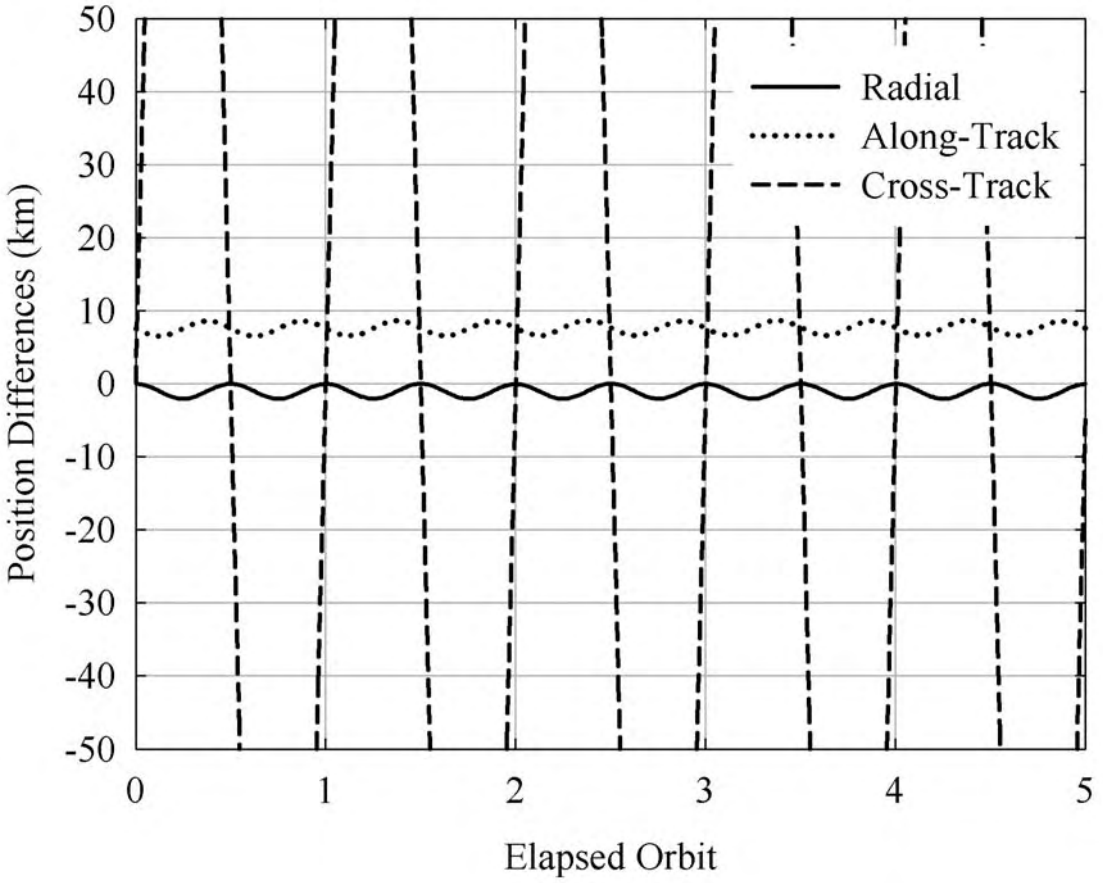

Figure 6. Three components at the separation vector between the two lower pair satellites during Phase-1.

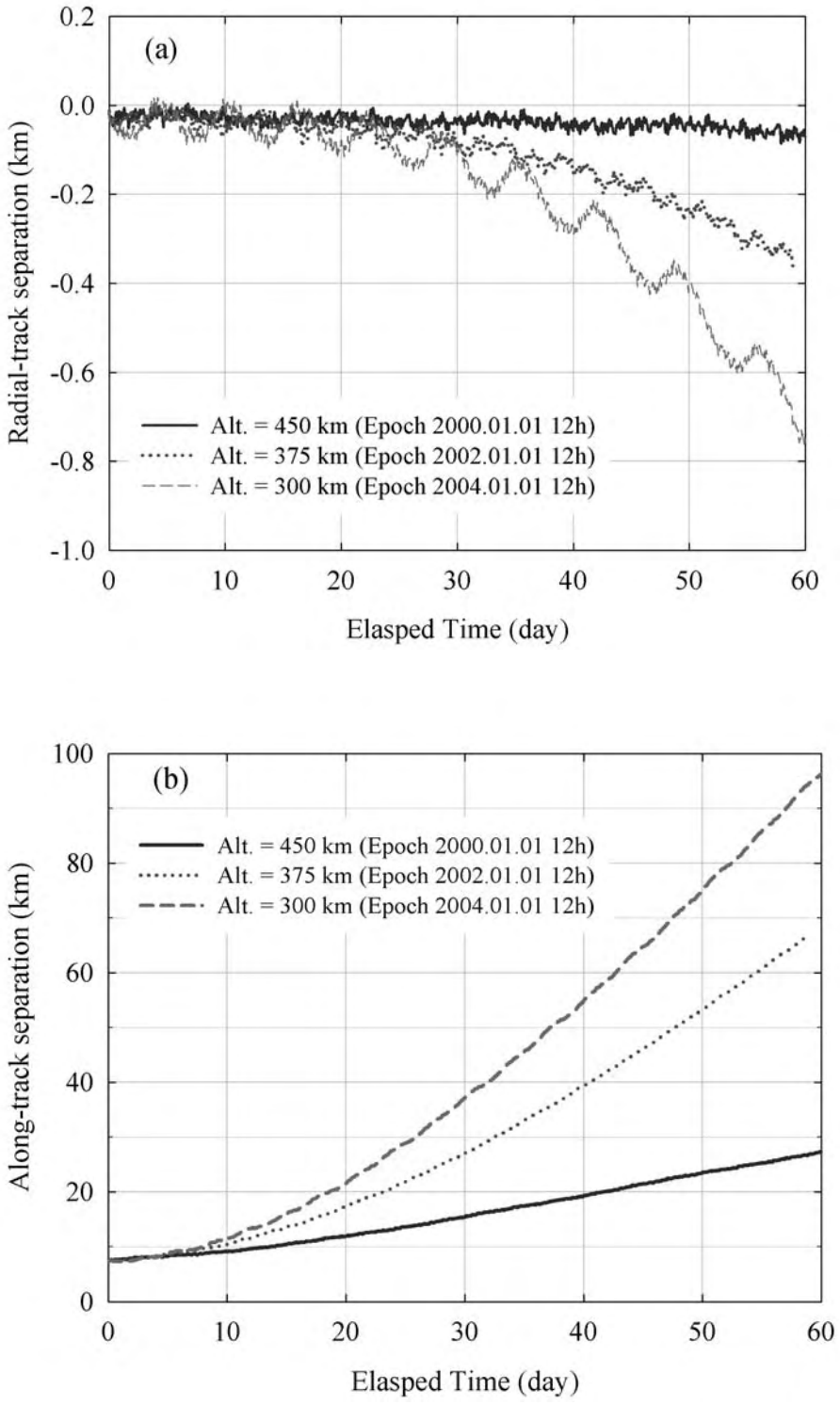

Figure 7. Radial and along-track separation of the lower pair satellites during the three phases; (a) radial separation near North Pole and (b) along-track separation near the equator.

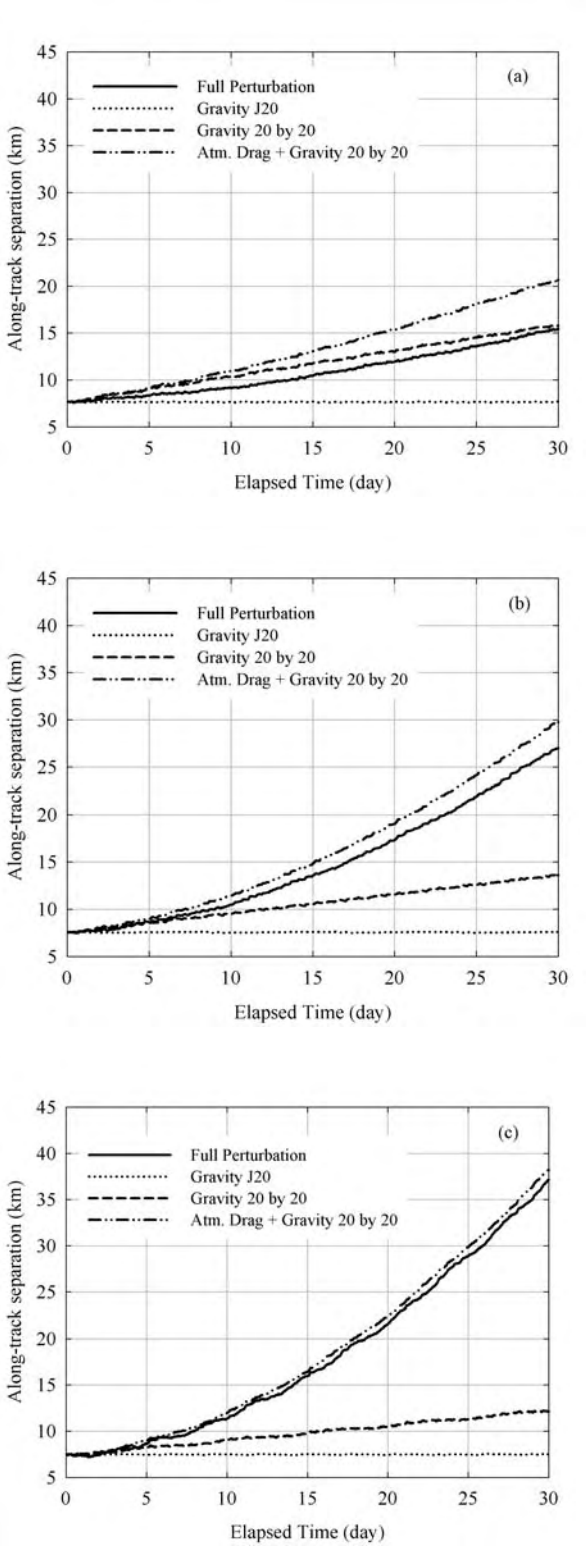

Figure 8. The effects of various perturbations on the along-track drift during the three mission phases; (a) Phase-1, (b) Phase-2, and (c): Phase-3.

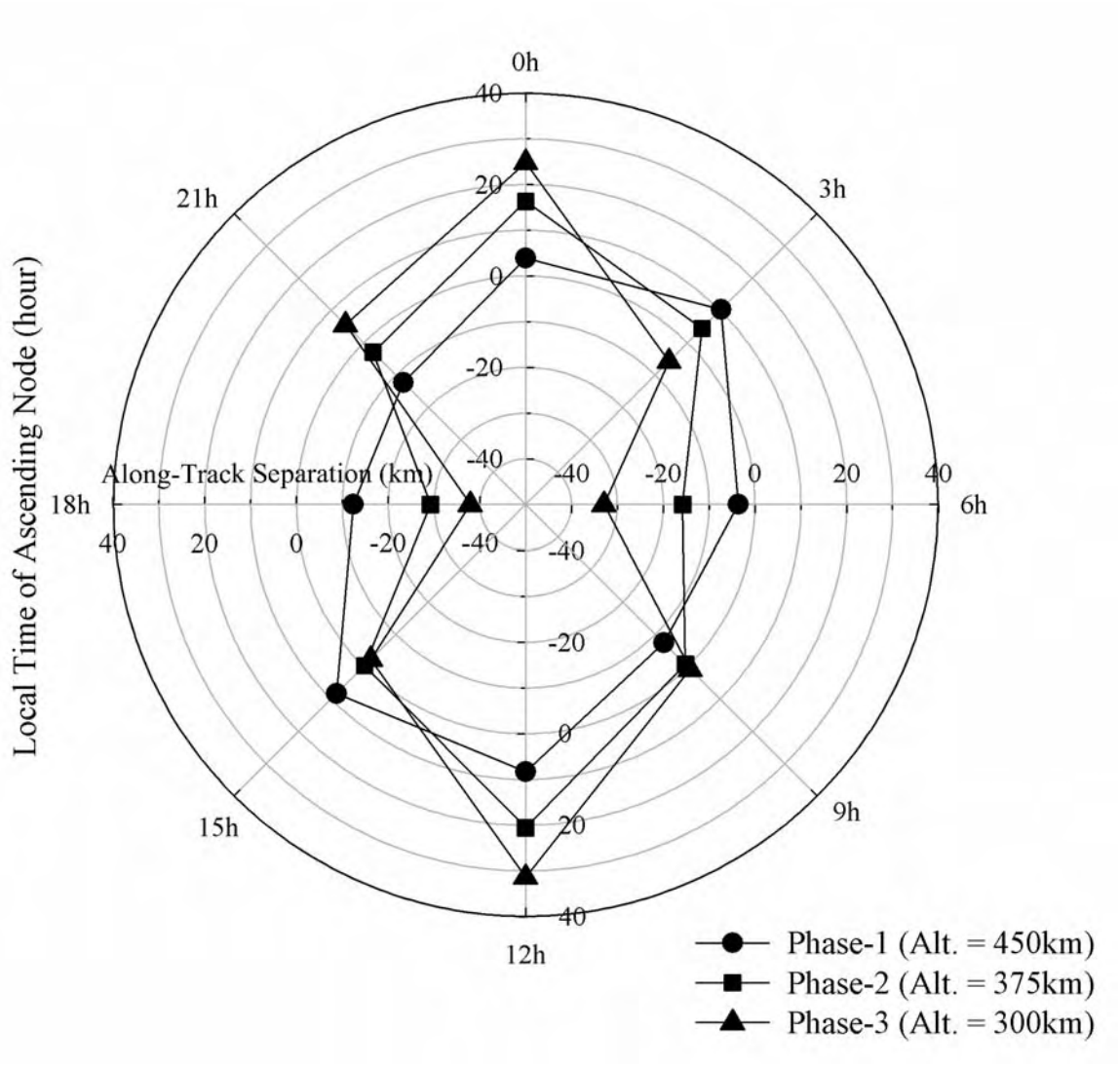

Figure 9. Along-track drift dependence on the local time of ascending node. The along-track drift is the value after 30 days of orbit simulation, and S/C A is ahead of S/C B for positive distances.

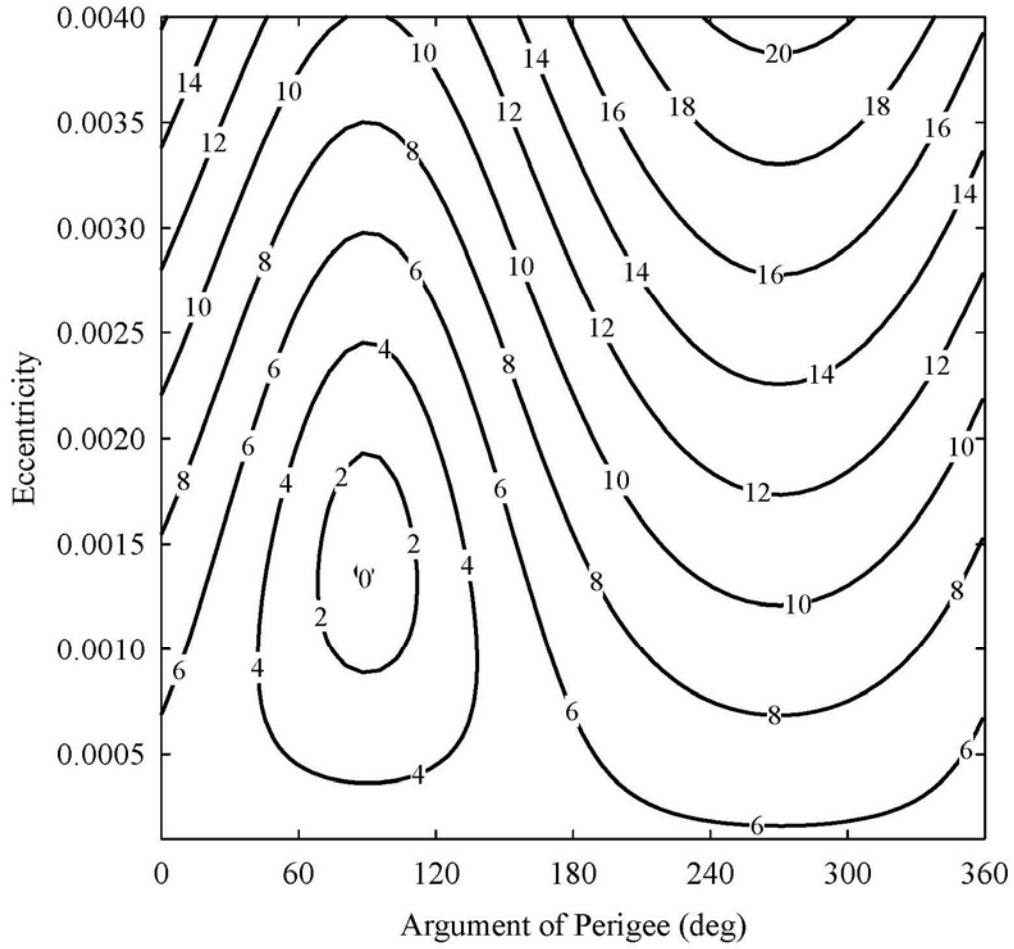

Figure 10. The minimum velocity change required for maneuvering the spacecraft into the frozen condition orbit using the single-impulse method during Phase-1. The numbers give the required $\Delta v_{\min}$ in units of m/s.